

Elliptic and Triangular Flow of Quark-Gluon Plasma in Pb+Pb Collisions in the sPHENIX Detector

Ziru Chen¹, Ye Liu^{2*}

¹*Qingdao Academy, Qingdao, China*

²*University of Minnesota, Minneapolis, USA*

**Corresponding Author. Email: liu01617@umn.edu*

Abstract: This paper presents the analysis of the hydrodynamic properties of Quark-Gluon Plasma (QGP) in Pb+Pb collision events collected by the sPHENIX detector, focusing on the elliptic flow (v_2) and triangular flow (v_3) by analyzing azimuthal angle distribution of particles. The two-dimensional correlation function between azimuthal angle difference ($\Delta\phi$) and pseudorapidity difference ($\Delta\eta$) that excludes collision pairs with $|\Delta\eta| < 1$ was analyzed. The shape of the graph suggests the hydrodynamic flow during Pb+Pb collisions explicitly. The value of $\langle v_2 \rangle$ and $\langle v_3 \rangle$ were compared with the value of the weighted average of eccentricity (ϵ_2) and triangularity (ϵ_3) with the same centrality (40–50%) of the simulated dataset generated by the PHOBOS Glauber Monte Carlo (Glauber MC) code. The trend of elliptic flow and triangular flow as a function of transverse momentum of the experimental data was also examined, and general increasing trends that agree well with that predicted by a multi-phase transport model (AMPT) were found.

Keywords: Quark-Gluon Plasma, elliptic flow, triangular flow, a multi-phase transport model, PHOBOS Glauber Monte Carlo.

1. Introduction

The study of elliptic flow in high-energy heavy-ion collisions, such as Pb+Pb collisions, is essential for understanding the properties of the quark-gluon plasma (QGP), a state of matter believed to exist shortly after the Big Bang. One of the key observables in these collisions is the elliptic flow, characterized by one-half of the second Fourier coefficient of the $\Delta\phi$ distribution v_2 , which provides insights into the initial geometry and the subsequent hydrodynamic expansion of the QGP.

Previous studies have shown that the Fourier coefficients of the $\Delta\phi$ distribution are sensitive to the initial geometry of the collision and the subsequent hydrodynamic evolution of the system. For instance, Alver and Roland (2010) discussed the role of collision-geometry fluctuations in generating triangular flow, quantified by the third Fourier coefficient v_3 [2]. Their findings highlighted the importance of understanding both v_2 and v_3 to gain a comprehensive picture of the QGP dynamics. Hence, the studying of advanced algorithms on prediction of the initial geometry of heavy-ion collisions is essential for research of the QGP dynamics.

One of the models that has been widely used to describe the initial geometry is The Glauber model. This model provides a framework for calculating quantities such as the number of participant nucleons (N_{part}) and the number of binary collisions (N_{coll}), which are crucial for interpreting flow

measurements. Miller et al. (2007) reviewed the application of the Glauber model in high-energy nuclear collisions and emphasized its relevance for flow studies [1].

In addition to the Glauber model, the A Multi-Phase Transport (AMPT) model also plays a significant role in understanding the dynamics of heavy-ion collisions. The AMPT model incorporates both the initial partonic and the hadronic phases, allowing for a comprehensive simulation of the collision process. Lin et al. (2005) demonstrated the effectiveness of the AMPT model in addressing the non-equilibrium effects experienced by particles with high transverse momentum (p_T) [3]. This model provides valuable insights into the development of hydrodynamics flow and the interactions within the QGP. With the prediction of those two models, the real data collected from Pb+Pb collisions are analyzed and compared.

Our study aims to analyze the elliptic and triangular flow in Pb+Pb collisions using data collected by the sPHENIX detector. By examining the $\Delta\phi$ distribution, $v_2(p_T)$, and $v_3(p_T)$, we aim to gain a deeper understanding of the hydrodynamic properties of the QGP. The results from our experimental data are compared with predictions from the PHOBOS Glauber Monte Carlo model and the AMPT model, providing a comprehensive overview of the flow dynamics in these collisions.

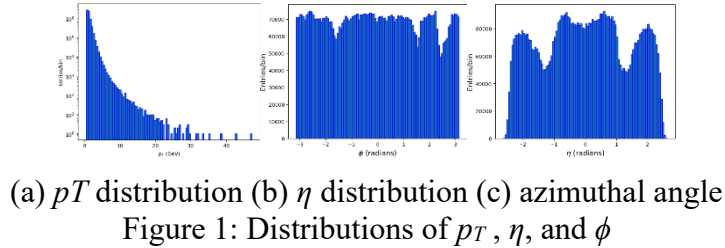
2. Analysis of azimuthal correlations

The sPHENIX detector, located at the Relativistic Heavy Ion Collider (RHIC), offers high precision data of Pb+Pb collisions to study. This dataset includes measurements of the transverse momentum (p_T), pseudorapidity (η), and azimuthal angle (ϕ) of particles produced in Pb+Pb collisions.

2.1. Raw data

The initial step of our analysis involved processing the raw data obtained from the sPHENIX detector. Those fundamental quantities are essential for understanding the behavior of particles under the extreme conditions created in heavy-ion collisions.

We visualized the distributions of these variables to gain initial insights into the data. Figure 1 presents the histograms of p_T , η , and ϕ , respectively.



The p_T distribution, shown in Figure 1. (a), expresses a characteristic inverse power-law shape, which is typical for heavy-ion collisions. This distribution indicates that many particles are produced with low p_T , while only a few gain high p_T .

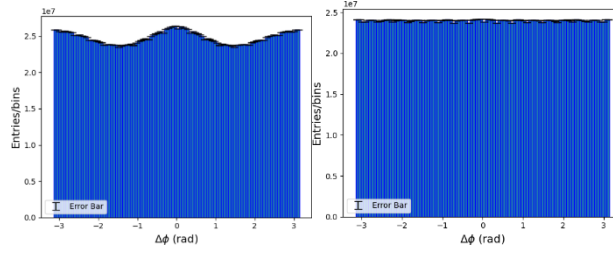
The η distribution in Figure 1. (b) demonstrates the spread of particles along the beam axis, which are expected to be approximately symmetric around $\eta = 0$. This symmetry reflects the balanced nature of the collisions, where particles spread evenly in both directions relative to the central collisions point.

Lastly, depicted in Figure 1. (c), the ϕ distribution exhibits the angular spread of particles in the transverse plane. The valleys in the distribution can be attributed to the non-uniform acceptance and efficiency of the detector.

2.2. 1-Dimensional correlation function of $\Delta\phi$

In order to explore the azimuthal correlations of particles produced in the Pb+Pb collisions, we analyzed the $\Delta\phi$ distributions for same-event pairs and mixed-event pairs. The $\Delta\phi$ distribution exhibits the differences in the azimuthal angle ϕ between pairs of particles.

Figure 2 shows the $\Delta\phi$ distributions for same-event pairs and mixed-event pairs. The same-event $\Delta\phi$ distribution exhibits a pronounced peak around $\Delta\phi = 0$, indicating a strong azimuthal correlation among particles produced in the same collision event. This peak suggests that particles are preferentially emitted close to each other in azimuthal angle, reflecting the hydrodynamic flow within the QGP



(a) $\Delta\phi$ distribution of same- event pairs (b) background $\Delta\phi$ distribution of mixed-event pairs.

Figure 2: $\Delta\phi$ distribution of same-event pairs and mixed- event pairs

On the other hand, the mixed-event $\Delta\phi$ distribution, which serves as a background reference, shows a much flatter distribution without a pronounced peak. Mixed- event pairs are constructed by combining particles from different events, which is typically used for reducing back- ground noise and correcting for acceptance effects. A method similar to that mentioned in [4] was applied to investigate the elliptic flow, which is using the correlation function. The background-subtracted correlation function is given by:

$$C(\Delta\phi) = \frac{S(\Delta\phi)}{B(\Delta\phi)} \quad (1)$$

where $S(\Delta\phi)$ is the same-event distribution and $B(\Delta\phi)$ is the mixed-event distribution. By using this equation, we normalize the same-event distribution by the mixed- event distribution to form the correlation function, which corrects non-physical correlations and acceptance effects.

2.3. Fitting function of $\Delta\phi$ correlation function

To quantify the azimuthal correlations observed in previous analysis, we fit the $\Delta\phi$ distribution to a Fourier series. The Fourier decomposition allows us to extract the flow coefficients, which characterize the strength of azimuthal anisotropies in particle emission. Specifically, we focus on the second and third Fourier coefficients, corresponding to elliptic and triangular flow, respectively.

The Fourier series used for fitting the $\Delta\phi$ Distribution is given by:

$$f(\phi) = k(1 + 2v_2^2 \cos(2\phi) + 2v_3^2 \cos(3\phi)) \quad (2)$$

where v_2 and v_3 represent the magnitudes of elliptic and triangular flow, and k is a normalization factor.

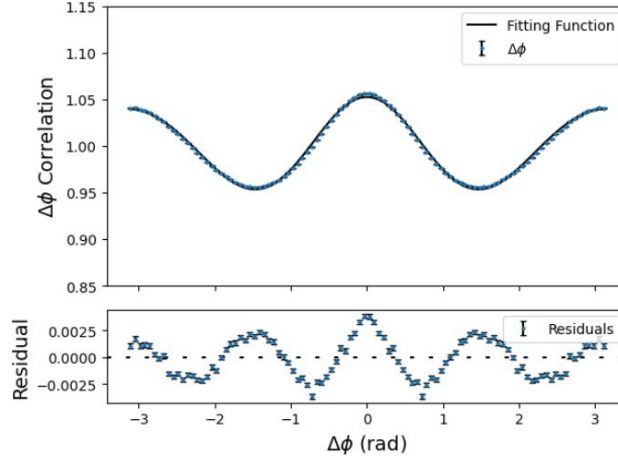


Figure 3: Fitting function and fitting residual of $\Delta\phi$ correlation function

Figure 3 shows the fitted function to the $\Delta\phi$ distribution and the corresponding residuals. The fitted function captures the main features of the $\Delta\phi$ distribution, with the v_2 and v_3 coefficients providing a measure of the strength of the elliptic and triangular flow. The periodic pattern of fitting residual indicates that higher orders of hydrodynamic flow also exist in heavy ion collisions, though their contribution is relatively small compared to v_2 and v_3 . However, it is a reasonable approximation to only consider the elliptic flow and triangular flow as the residual has a negligible magnitude.

2.4. 2-Dimensional correlation function of $\Delta\phi$ and $\Delta\eta$

To further investigate the azimuthal and longitudinal correlations between particles, we constructed the 2- dimensional correlation function of $\Delta\phi$ and $\Delta\eta$. The $\Delta\phi$ represents the azimuthal angle difference between particle pairs, while $\Delta\eta$ denotes the pseudorapidity difference.

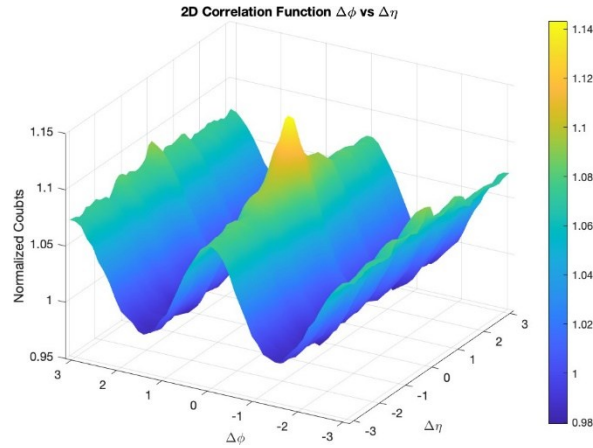


Figure 4: 2D correlation function of $\Delta\phi$ and $\Delta\eta$

In Figure 4, the noteworthy peak at the origin points indicates a strong correlation among particles emitted close to each other in both azimuthal angle and pseudorapidity. This peak is a signature of collective flow in the QGP, where particles exhibit collective behavior due to the high energy density and strong interactions within the plasma. In addition, the narrow peak in $\Delta\eta$ suggests that particles are emitted over a short range in pseudo-rapidity.

2.5. Excluding collision pairs with $|\Delta\eta| < 1$

After plotting the 2-dimensional and 3-dimensional $\Delta\eta$ versus $\Delta\phi$ correlation functions, it can be observed that the peak at (0,0) is contributed by both the trigonometric shape of $\Delta\phi$ distribution and the triangular shape of $\Delta\eta$.

Table 1: Fit parameters v_2 and v_3 for the whole dataset and the filtered dataset

Dataset	v_2	v_3
Original	0.151348 ± 0.000393	0.056909 ± 0.001045
Filtered	0.147003 ± 0.000518	0.051683 ± 0.005142

Therefore, collision pairs with $|\Delta\eta| < 1$ should be excluded since they are unrelated to hydrodynamic expansion. The $\Delta\phi$ correlation function, its fitting function, and the fitting residual for collision pairs with $|\Delta\eta| < 1$ are shown in Fig. 5.

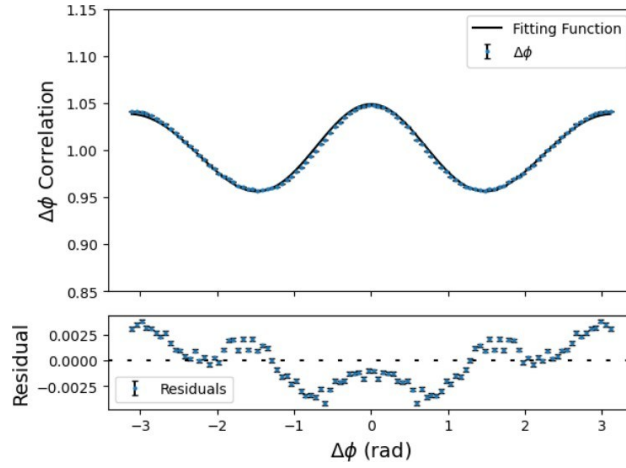


Figure 5: Fitting function and fitting residual of $\Delta\phi$ correlation function excluding pairs with $|\Delta\eta| < 1$

After excluding pairs that are irrelevant to the hydrodynamic flow in QGP, v_2 and v_3 decrease as shown in the Table 1, as well as the height of the peak at $\Delta\phi = 0$ on the residual plotting, suggesting that the influence of the factor unrelated to hydrodynamic flow reduces as expected.

3. Hydrodynamic flow as a function of transverse momentum

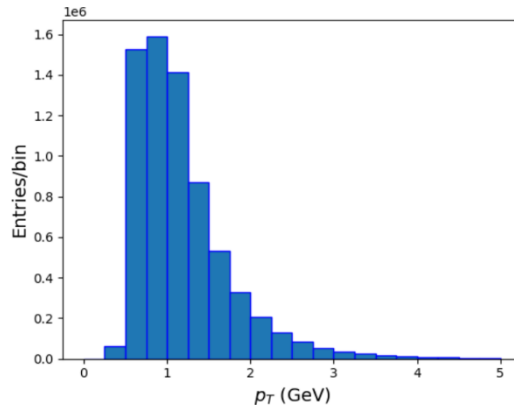
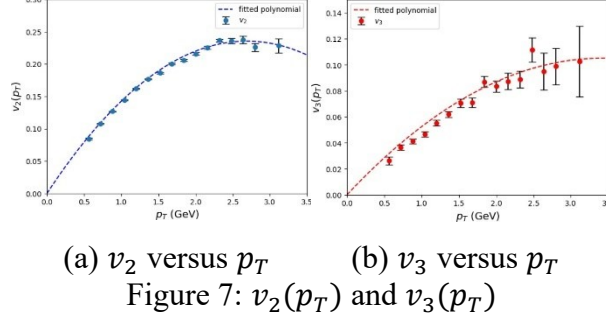
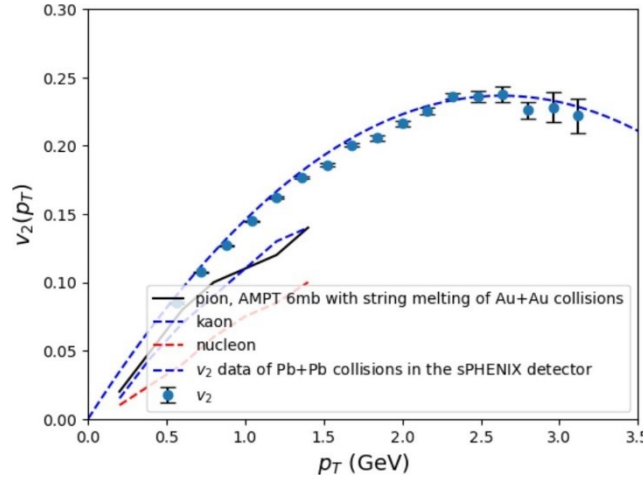


Figure 6: p_T distribution from 0 to 5 GeV

The p_T distribution from 0 to 5GeV is presented in Fig. 6. After plotting the p_T distribution of all particles from 0 to 5GeV in bins of 250MeV , we chose the p_T range from 0 to 3.2GeV to analyze the trend of v_2 and v_3 since insufficient events outside this range may lead to high uncertainty in data points.



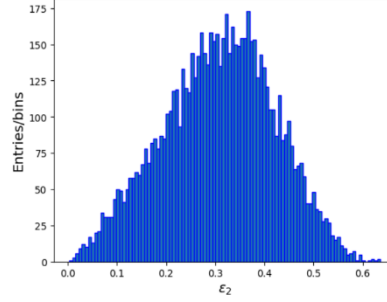
From the v_2 versus p_T and v_3 versus p_T graphs shown in Fig. 8, in general, it is evident that both the elliptic flow and triangular flow become more significant as p_T increases and level off at large p_T values. This trend agrees with past research, such as the analysis of v_2 as a function of p_T of Xe+Xe and Pb+Pb collisions at the Large Hadron Collider, and Ru+Ru and Zr+Zr collisions in experiments run at $\sqrt{s_{NN}} = 200\text{GeV}$ at the RHIC by the STAR collaboration. [6, 7] In Fig. 9, the curves shown in the range of $0.15\text{ GeV} < p_T < 1.4\text{ GeV}$ are results predicted by the AMPT model for minimum-bias Au+Au collisions at $\sqrt{s_{NN}} = 200\text{GeV}$ and $|\Delta\eta| < 1$ with string melting and using 6 mb for the parton scattering cross section.[3] It can be observed from the graph that the trends of $v_2(p_T)$ and $v_3(p_T)$ in Pb +Pb collisions at lower transverse momentum values are similar to the results for Au +Au collisions predicted by the AMPT model.



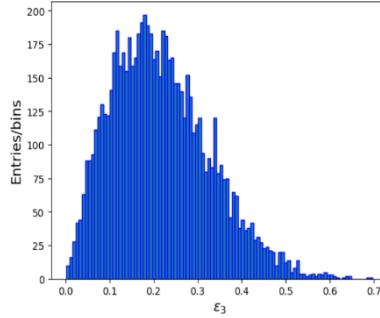
4. Comparison with the phobos glauber monte carlo model

Glauber model is widely used for analyzing geometric quantities in the initial state, typically represented by the impact parameter (b), number of participating nucleons (N_{part}), and number of binary nucleon-nucleon collisions (N_{coll}). [1] The Monte Carlo approach of the Glauber model is useful due to its simplicity in calculating geometric quantities, such as N_{part} and N_{coll} , and the possibility to simulate measurable variables in experiments. [1] In this research, we applied the PHOBOS Glauber Monte Carlo code available online to generate a simulated dataset containing 75000 Pb+Pb collision events in order to compare the experimental results with theoretical predictions.

In previous literature, it is found that $\langle v_2 \rangle(\epsilon_2)$ and $\langle v_3 \rangle(\epsilon_3)$ are linear functions in collision events generated by the Glauber Monte Carlo simulation.[2] Therefore, it is meaningful to compare v_2 and v_3 of the experimental data with ϵ_2 and ϵ_3 of the simulated data. The centrality of our set of experimental data is 40–50%, so only events with the same centrality in the dataset generated by the Glauber MC code were considered when making comparisons. The average value of the number of participant nucleons (N_{part}) is approximately 143. 635, and thus it would be reasonable to compare with results where $160 < N_{part} < 200$ in previous literature. [2]



(a) Distribution of ϵ_2 with centrality 40–50 %



(b) Distribution of ϵ_3 with centrality 40–50 %

Figure 9: Distribution of ϵ_2 and ϵ_3 with centrality 40–50 percent

From the calculation of the weighted average of v_2 and v_3 , one point on each of the average v_2 versus average ϵ_2 and average v_3 versus average ϵ_3 graph can be obtained, which are $(\langle \epsilon_2 \rangle, \langle v_2 \rangle) = (0.306824, 0.147719)$ and $(\langle \epsilon_3 \rangle, \langle v_3 \rangle) = (0.216565, 0.051076)$. Our results provide more data to support the scaling law between the elliptic flow normalized by the inverse of the Knudsen number and eccentricity. [6]

5. Uncertainty analysis

Even though the sPHENIX detector of the RHIC has a nearly 4π solid-angle acceptance, the pair acceptance effects have to be taken into account when analyzing the correlation function of $\Delta\phi$, which is observed from Fig. 1 (c). [4] In this research, the correlation function is calculated by dividing the distribution of $\Delta\phi$ of particles in the same event by the mixed-event background distribution to reduce the influence of pair acceptance effects and random background. The v_2 and v_3 values of the $\Delta\phi$ correlation function with $|\Delta\eta| > 1$, which are 0.147003 ± 0.000518 and 0.051683 ± 0.005142 , have 0.352374% and 9.94911% percentage uncertainties respectively.

In addition, collision pairs with $|\Delta\eta| < 1$ were excluded from our analysis of v_2 and v_3 to reduce impacts of factors unrelated to hydrodynamic expansion. Besides, when analyzing $v_2(p_T)$ and

$v_3(p_T)$, only particles with $0\text{GeV} < p_T < 3.2\text{GeV}$ were considered to reduce uncertainties caused by the insufficient number of particles at high transverse momentum.

6. Summary

In this study, the $\Delta\phi$ correlation function of Pb+Pb collision pairs was analyzed to investigate the elliptic flow and triangular flow in the QGP. In particular, we focused on the trend of $v_2(p_T)$ and $v_3(p_T)$ and compared our results with that predicted by the AMPT model. Our findings support the previous evidence that $v_2(p_T)$ and $v_3(p_T)$ show increasing trends at low transverse momentum values and eventually level off as p_T increases. [3] In addition, previous research mostly focused on $v_2(p_T)$ and $v_3(p_T)$ at $|\Delta\eta| < 1$. Therefore, our analysis of $v_2(p_T)$ and $v_3(p_T)$ at $|\Delta\eta| > 1$ could provide a more comprehensive understanding of the hydrodynamic properties of QGP. Finally, we also compared the weighted average of v_2 and v_3 with the average value of ϵ_2 and ϵ_3 of the data generated by the PHOBOS Glauber Monte Carlo code.

Acknowledgement

Ziru Chen and Ye Liu contributed equally to this work and should be considered as co-first authors.

References

- [1] Michael L. Miller, Klaus Reygers, Stephen J. Sanders, Peter Steinberg, Glauber Modeling in High Energy Nuclear Collisions, *Ann. Rev. Nucl. Part. Sci.* Vol. 57, 205-243 (2007).
- [2] B. Alver and G. Roland, Collision-geometry fluctuations and triangular flow in heavy-ion collisions, *Phys. Rev. C* Vol. 81, 039903 (2010).
- [3] Lin, Zi-Wei and Ko, Che Ming and Li, Bao-An and Zhang, Bin and Pal, Subrata, A multi-phase transport model for relativistic heavy ion collisions, *Phys. Rev. C* Vol. 72, 064901 (2005).
- [4] CMS Collaboration, Long-range and short-range dihadron angular correlations in central PbPb collisions at a nucleon-nucleon center of mass energy of 2.76 TeV, *JHEP* Vol. 7, 76 (2011).
- [5] B. Alver and M. Baker and C. Loizides and P. Steinberg (2008), The PHOBOS Glauber Monte Carlo.
- [6] Moriggi, L. S. and Rocha, V. E. S. and Machado, M. V. T., Study of the azimuthal asymmetry in heavy ion collisions combining initial state momentum orientation and final state collective effects, *Phys. Rev. D* Vol. 108, 074013 (2023).
- [7] Sinha, P. (2024), Probing Nuclear Structure Using Elliptic Flow of Strange and Multi-strange Hadrons in Isobar Collisions., In: Jena, S., et al. *Proceedings of the XXV DAE-BRNS High Energy Physics (HEP) Symposium 2022*, 12-16 December, Mohali, India.